Heat and Technology
Vol. 32, n. 1-2, 2014

CONTRIBUTION TO THE STUDY OF MECHANICAL PROPERTIES OF HIGH DENSITY POLYETHYLENE (HDPE) UNDER THE EFFECT OF TEMPERATURE AND MODELING OF ITS BEHAVIOUR AT 60°C

Sofiane Sadoun*, Ali Gasmi*, Nasser Eddine Zeghib°, Ali Yousfi*

Laboratoires de : * Physique du solide (LPS), °Mécanique des Matériaux et Maintenance Industrielle (LR3MI)
Badji Mokhtar University, BP12, Annaba 23000, Algeria.
E-mail : sofsadoun@yahoo.fr

ABSTRACT

These high density polyethylene samples (HDPE) were subject to a uniaxial tension under the influence of temperature ranging from 20 to 120°C at a constant stretching speed of 50mn/mn and at various stretching speeds of 50 to 800mn/mn for a constant temperature of 60°C. The material has shown various mechanical behaviors resulting in various nominal curbs. The evolution of the mechanical magnitudes has been monitored based on the two mentioned external influences. We have shown the analogy of the effect of the temperature decrease and the speed increase. In order to transform the nominal curbs into true curves, we have assumed a relation whose implementation has given a good compliance with the bibliographical research. By selecting the curve achieved a 60°C for a stretching speed of 50mn/mn with the assumption that the polymer is isotropic, the plain deformation homogenous perfect plastic and for a triaxibility coefficient $F_T = 1{,}0877$; the implementation of Von Mises relations has allowed us to complete an effective curb. The latter has given a good compliance with the multiplicative curve, modeled according the G'SELL law.

Key words: HDPE, mechanical properties, true curb, effective curb, modeling.

1. INTRODUCTION :

Polyethylene (PE) is a semi crystalline thermoplastic of the polyolefin family. It has a very simple chemical structure [1] achieved by ethylene polymerization C_2H_4, resulting in macromolecules composed of the repetition of monomer motif CH_2-CH_2 [2, 3]. Its consumption in the international market is considerable due its low cost manufacture and its physical and mechanical properties along with various uses in the day life [4]. In 2008; the PE alone, represented a quarter of the synthetic polymer production assessed at 245 million tons [2]. The statistics show [5] that more than 90% of the transport pipelines and gas distribution newly installed in throughout the world are exclusively made of Polyethylene (PE) due to its good performances. According to the methods used for the ethylene polymerization, various types of Polyethylene can be achieved: various chain structures, various physical and mechanical structures and various solid structures [6] such as: the high density (HDPE), low density (LDPE), linear low density (LLDPE), low molecular weight (PEBPM) and ultra high molecular weight (PEUHPM) polyethylenes. Since it was discovered in 1953 by the German chemist Karl Ziegler, high density polyethylene (HDPE) was given a double attention. Considered as a model for the scientific study of the semi crystalline polymers and innovating, replacing therefore certain traditional material such steel, and cast iron in the advanced applications [2]. Its linear structure with a zigzag configuration [1, 7], does not include any short ramification and any very weak long branches, a motif CH_2-CH_2 and 28 g/mol molar mass [7]. It is achieved by low pressure ethylene polymerization processes, alone or with co monomers (Philip and Ziegler processes). Its main uses are: packaging, cable coating, fuel tanks, bullet proof vests, pipe manufacturing for gas and liquid transportation. Its main qualities are: low water sensitivity, water steam proof, excellent electrical properties and even low temperatures resilience [8]. Its various phases are: orthorhombic, discovered by BENN in 1939, is the most stable and the most common; achieved at normal temperature and pressure conditions $295<T<373$°K, $0<P<2{,}5$ GPa [9, 10,11]. Hexagonal phase is achieved for high pressures and temperatures above 0,3 GPa and 200°C [12]. It is partially disordered, intermediate between the orthorhombic phase and the liquid state [13]. In this grid, the chains are drawn and the density is too high [14]. The monoclinic phase is achieved under strong cold deformation or during very low temperature crystallization [14, 15]. This phase is metastable and shifts into an orthorhombic just above the PE fusion point at an ambient pressure [16].

Certain authors [17] were interested in the modification of the PE crystalline phases under the influence of a high pressure. The interval was between 0 and 40 GPa for a temperature of 280°C. They have noticed that there are three phases

depending on the pressure increase. One is orthorhombic thermodynamically stable until around 6 GPa. If exceeded it reversibly shifts into a metastable monoclinic phase. Another monoclinic phase transition will occur between 14 and 16 GPa.

It is known that the mechanical tests are indispensable for the user in order to determine the material characteristics to optimize its utilization. The tensile is frequently used and considered to be the simplest test. It consists of testing a sample and measuring its elongation. A simple curve (stress-deformation) will be a good base element in order to know the mechanical behavior of a given material. For polymers, the mechanical behaviors are related to the experiment external conditions. The properties are more sensitive than those metals exposed to external influences such as temperature, the test duration, the intensity and the loading type, chemical agents [7,8] and the ultra violate radiation (UV) [7,14,18]. Among the latter, test duration (strain rate or stretching speed) and temperature are the most influent. The external influences have also roles in structure and microstructure macromolecular chains of polymers (damage effect example). The majority of mechanical structures are subject, not only to mechanical loads but also to variable thermal solicitations [19].

This study aims at studying the evolution of the HDPE mechanical processes subject to the uniaxial tensile under the effect of a range of temperature and various stretching speeds and modeling its mechanical behavior at a selected temperature of 60°C.

2. EXPERIMENTAL STUDY:

The HDPE sample (polymerized according to Philips process) processed in this study was provided by POLYMED Company. The experiments were carried out at the Laboratory of Physics and Mechanics of Materials (LPMM) of Metz University (France). The material tested was under the form of various identical samples, plains and homogenous. Its characteristics are shown in table 01:

Table 01: High density polyethylene characteristics

Physical Magnitude	Numerical Value
Sample initial length l_0	95,21 mm
Sample initial thickness a_0	13,5 mm
Sample initial width b_0	3 mm
Glass transition temperature T_g	-125 °C
Melting temperature T_m	134,4 °C
density ρ	0,96 g/cm^3
volume mass m_v	1 g/cm^3
Degree of crystallinity χ	75%

Our tests were carried out on a ZWICK type tensile machine equipped with a furnace driven by a testxpert software version 11.01 (V11.01), capable of providing during the test t(s), the sample elongation Δl (mm) (gages deformation measurement), its stretching strength F (N) and to transfer the results to the Excel software. Testxpert is universal testing software used since 1996 on material components and fine pieces. The testxpert utilization range covers the traditional testing machines of ZWICK range (tensile machines, compression, flexion and universal machines).

The HDPE underwent various temperatures T (from 20 to 120°C) at a constant stretching speed (50mn/mn) then at stretching speed range s (from 50 to 800mm/mn) at a constant temperature (60°C).

3. RESULTS AND OBSERVATIONS:

We have obtained various nominal curves (stress - deformation) $(\sigma_n - \varepsilon_n)$ (figures 01 and 02) shown as follows:

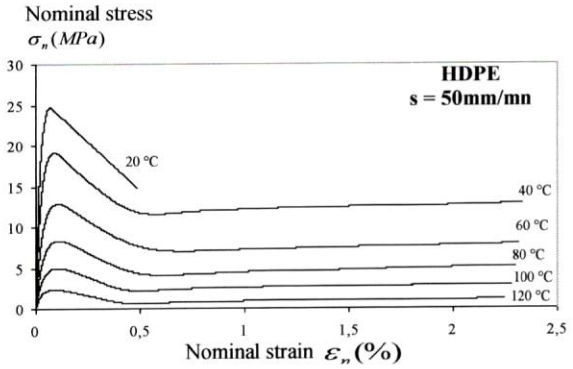

Figure 01: HDPE nominal curves (stress- strain) ($\sigma_n - \varepsilon_n$) under temperatures ranging from 20 to 120°C at 50 mm/mn

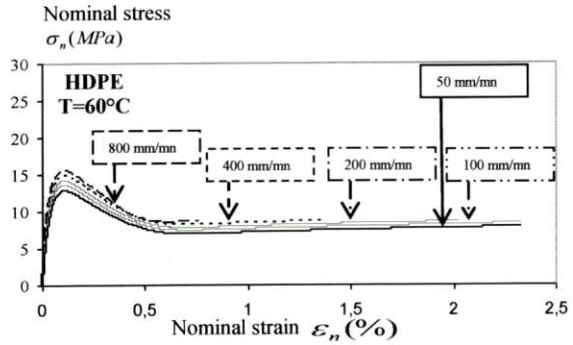

Figure 02: HDPE nominal curves (stress- strain) ($\sigma_n - \varepsilon_n$) under stretching from 50 to 800mm/mn at 60°C

Note that:

The nominal stress σ_n was calculated according to the relation (1):

$$\sigma_n = \frac{F}{S_0} \qquad (1)$$

Where: $S_0(mm^2) = a_0 \times b_0$, sample initial section.

The nominal strain ε_n was calculated according to the relation (2):

$$\varepsilon_n = \frac{\Delta l}{l_0} \qquad (2)$$

Based on the curves shown hereunder, we note that:

- For each temperature value T (at a constant speed), or at various speeds for a constant temperature, the material showed a particular normal curve (stress-strain) $(\sigma_n - \varepsilon_n)$, resulting in a particular mechanical behavior.
- For a same stretching speed, the curve feature decreases for a temperature elevation T. it otherwise increases for a speed elevation when the temperature is taken constant.
- The deformation level at failure $\varepsilon_{failure}$ changes with the two parameters T and s: The more the temperature is high or the speed is low, the more it is delayed.
- The failure did not occur for certain samples, and this until the machine furnace length is achieved (conditioning the experiment); example: curve at T= 40°C for a speed s = 50mn/mn.

4. ANALYSIS AND DISCUSSIONS:

Regardless of the experimental curve achieved, three different stages are distinguished:

- **1st stage:** the curve shows a reversible elastic deformation caused by the amorphous phase due to the fact that the module of this stage is largely lower than the crystalline phase [20, 21]. This slope curve shows the Young module $E(MPa)$, calculated based on the relation (3):

$$E(MPa) = \frac{\Delta\sigma}{\Delta\varepsilon} \qquad (3)$$

Where: $\Delta\sigma(MPa)$: stress variation, $\Delta\varepsilon$: deformation variation.
The curve initially linear brings out a certain non linearity just before the flow point (corresponds to the maximum) due to viscoelastic effects [20, 22]. The ordinate on axis y represents the stress at the flow point (tensile strength) $\sigma_{max}(MPa)$.

- **2nd stage:** the nominal stress lowers. It is only a geometrical effect as we do not take into consideration the sample section decrease which is not homogenous. It thins without failure. After initiation then situation aggravation, this plastic instability stabilizes then propagates to cover the entire length. The substance flow occurs at both ends of the restriction area through preferential polymer chains orientation.
- **3rd stage:** We witness a hardening along with a progressive increase of the flow stress and a final failure (not performed for all the samples).

5. RESULTS ANALYSIS:

For a further detailed study of the temperature and stretching speed influence on the HDPE behavior, we looked into the evolution of mechanical magnitudes shown as follows:

5.1 Magnitudes variation under temperature influence:

While it is possible to determine with good accuracy the metals elasticity limit, the plastic substances viscoelastic behavior often does not allow an accurate assessment of their elasticity limit [23]. By making grades in the elastic domains of the achieved curves, the values based on Y axis, which correspond to the linear section, show approximate values at the elastic limit $\sigma_{elastic}(MPa)$.

The figures (03, 04, and 05) respectively represent the Young module variations $E(MPa)$, tensile strength $\sigma_{elastic}(MPa)$ and elastic limit resistance $\sigma_{max}(MPa)$ under solicitation of temperature from 20 to 120°C at a constant stretching speed of 50mn/mn:

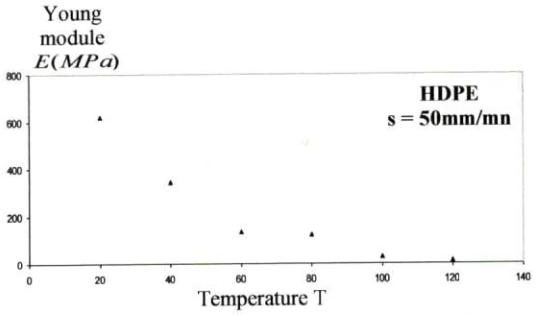

Figure 03: Young module variation under various temperatures at a constant stretching speed of 50mm/mn

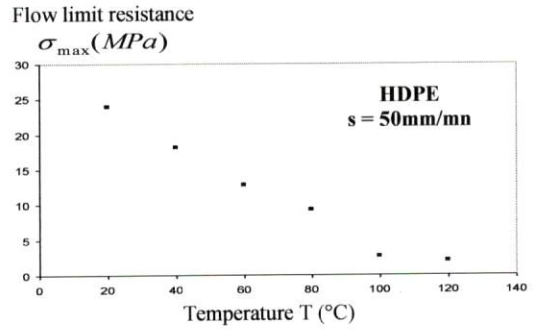

Figure 04: stress variation at flow limit under various temperatures at a constant stretching speed of 50mm/mn

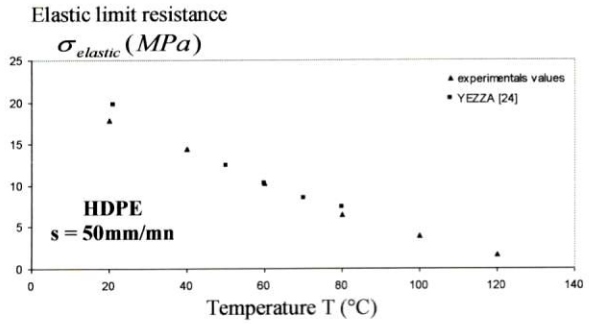

Figure 05: stress variation at elastic limit resistance under various temperatures at a constant stretching speed of 50mm/mn

5.2 Mechanical magnitudes variation under the effect of stretching speed:

The figures below (from 06 to 09) represent respectively the Young module $E(MPa)$, tensile strength $\sigma_{elastic}(MPa)$, elastic limit resistance $\sigma_{max}(MPa)$ and failure deformation level $\varepsilon_{failure}$ under the stretching speed solicitation at a constant speed of 60°C.

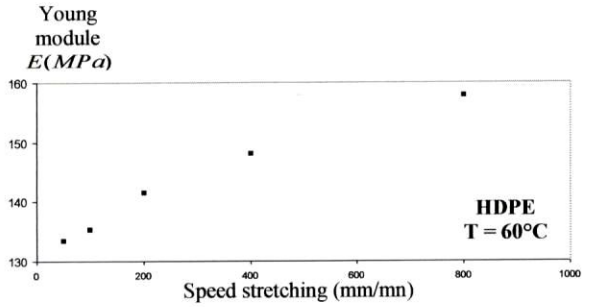

Figure 06: young module variation under various stretching speeds at constant temperature 60°C

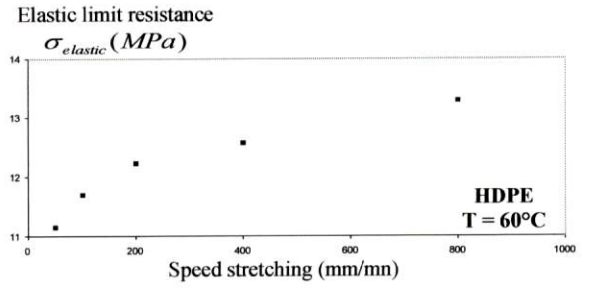

Figure 07: Stress variation at elastic limit under various stretching speeds at constant temperature 60°C

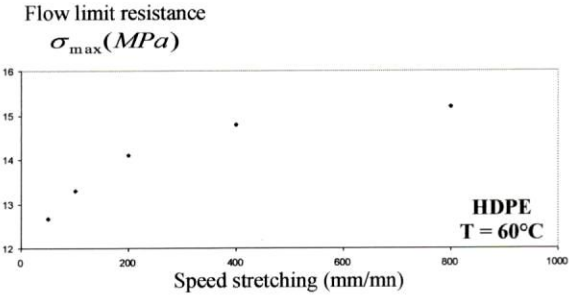

Figure 08: stress variation at flow limit under various stretching speeds at constant temperature 60°C

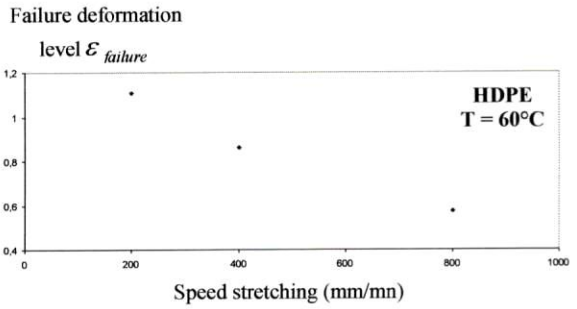

Figure 09: failure deformation level variation under various stretching speeds at constant temperature 60°C

According to the figures shown above, we notice that the mechanical magnitudes decrease for a temperature elevation. The same magnitudes increase for a stretching speed elevation (except for the failure deformation level).

6. INTERPRETATION:

Generally speaking the materials have an energy absorption phenomenon during tensile. The energy absorption capacity of a body is defined as the energy to be provided to cause its failure. This energy can be determined by integration from the area under the corresponding curve (stress-elongation) until the failure point. Inserted in the normalized section or in the studied sample volume, it is often defined as the material toughness [1]. A large area under the curve (stress-deformation) is equivalent to a high mechanical absorption capacity, contrary for a narrow area where the mechanical absorption capacity is low.

The polymers specific capacity is related to the fact that macromolecules do not always react instantly to a solicitation application [25]. The various consecutive molecular chains try to spread the imposed stresses by physically rearranging until reaching a balance position. If the applied solicitation is too rapid with respect to the molecules rearranging capacity, the polymer materials have a rigid and fragile behavior; this is related to the macromolecules inability to rearrange in an appropriate lap of time. In the opposite case, if the solicitation is slow, the same material show a ductile and flexible behavior due to the sufficient time allowing the molecular

chains to attain a balance position corresponding to the stresses underwent. [1]. Therefore, the polymers show a fragile behavior for a low temperature and a ductile behavior if subject to a high temperature. A temperature elevation break the polymers chain and increase the atoms vibrations movements, this facilitates the molecular rearrangements process (the HDPE is a thermoplastic material, the bonds between the macromolecules are of physical type, the latter are very sensitive to the heat).

7. PHYSICAL APPROACH OF THE OBTAINED CURVES:

In order to transform the nominal curves into true ones, we have the following equations (which are applicable only for a homogenous deformation).

$$\sigma_{v_1} = \sigma_n.(1+\varepsilon_n) \quad (4)$$

$$\varepsilon_v = \ln(1+\varepsilon_n) \quad (5)$$

In reality, the deformation is heterogeneous during the testing and occurs in the center of the sample (neck area) that the deformation is strong. After the reduction appearance, the deformation and the stress vary from a point to another in a deformed sample. Certain authors looked into studying the deformation in this environment [2, 27] in a representative volume element (V.E.R) with using a metric video piloting mechanical testing device (video traction) and obtained real curves (stress-deformation). According to these results, the volume does not remain constant during the deformation and there is a competition between the expansion effects and compaction in the macromolecular chains, which can be explained by the amorphous phase mobility, influenced itself by temperature and time.

Based on literature, the true curve (stress-deformation) of a semi crystalline polymer stretched in its rubber state environment ($T_{glass} \langle T_{experimental} \langle T_{melting}$) does not show a tensile hook [28, 29, 30] (figures10, 11 and 12). The elastic limit shows a progressive rounded transition [29].

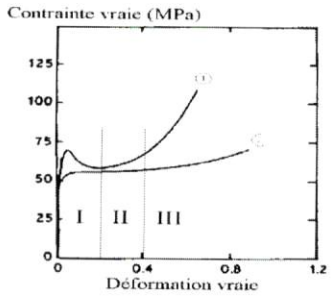

Figure 10: true stress typical evolution with true deformation in rubber state environment: (1) for amorphous polymer, (2) for semi crystalline polymer [28].

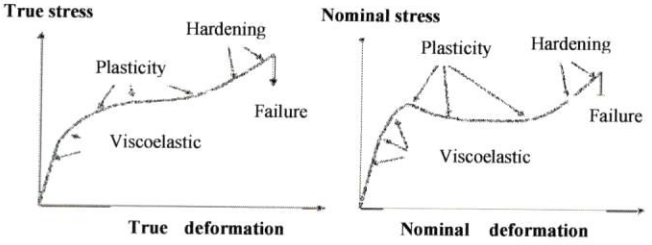

Figure 11: chronic curves (stress – deformation) represent the true mechanical behaviour (left) and nominal (right) of a semi crystalline polymer [29]

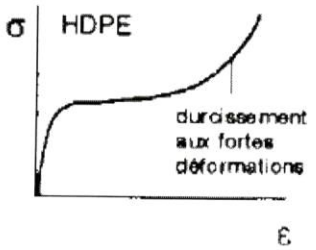

Figure 12: True curve (stress – deformation) for HDPE [30]

Since the outlined equations (4) and (5) are specific to the homogenous deformation these applications in our case brought out tensile hooks on the true curves (stress – deformation); we have assumed that the true curve meets the following relation:

$$\sigma_{v_2} = \sigma_n \exp(2\varepsilon_v) \quad (6)$$

In this paragraph, we have applied this relation for 60°C at a speed of 50mn/mn (figure 13) and it has given the same observations shown hereafter for all experimental temperatures and speeds.

If we do the two true curves superposition $\sigma_{v_1}, \sigma_{v_2}$, we notice that:

- In the elastic area the two curves are identical.
- In the viscoelastic area: small discrepancy between the two curves with $\sigma_{v_{2max}} \rangle \sigma_{v_{1max}}$.
- In the plastic area: the discrepancy between the two curves increases in terms of the true strain. Thus in the curve σ_{v_2}, we observe that:
  - First, there is a low stress variation whereas the material undergoes a substantial deformation in the neck area.
  - Then, a rapid stress increase along with a substantial sample deformation.

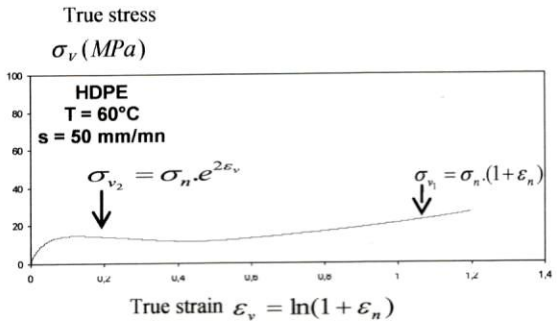

Figure 13: Tow true curves (stress – deformation) at T=60°C and s= 50mm/mn obtained according to tow different formulas

7.1 Relation between σ_{v_1} and σ_{v_2} :

$$\sigma_{v_2} = \sigma_n \exp(2\varepsilon_v) = \sigma_n[\exp(\varepsilon_v)]^2 = \sigma_{v_1}(1+\varepsilon_n) \tag{7}$$

$\Rightarrow (1+\varepsilon_n)$: Multiple value to have a true curve σ_{v_1} without a tensile hook during a semi crystalline polymer stretching in its rubber state.

7.2 Obtaining true curves:

The figures 14 and 15 represent the true curves obtained from nominal curves (figures 01 and 02) by applying the relations (05) and (06):

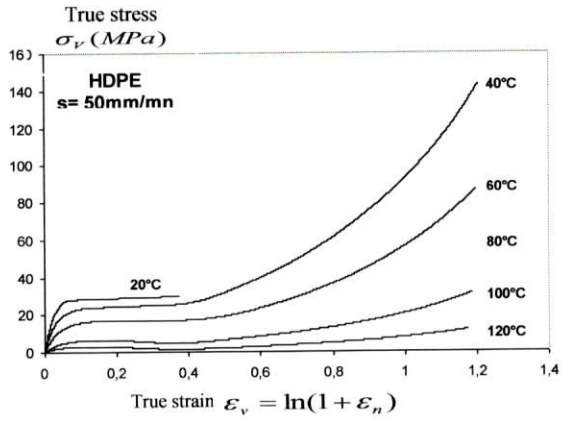

Figure 14: True curves (stress – deformation) of HDPE obtained from nominal curves for various temperatures at 50mm/mn

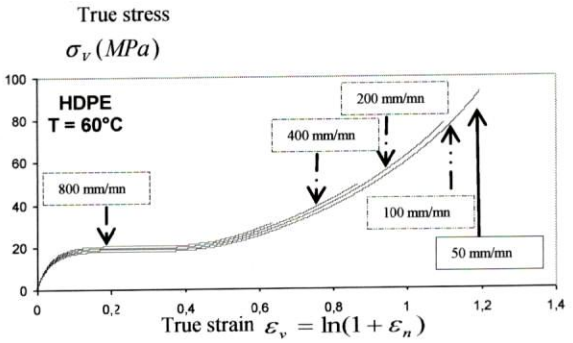

Figure 15: True curves (stress – deformation) of HDPE obtained from nominal curves for various stretching speeds at 60°C

According to the last figures (14 and 15), the shape of the various curves obtained is identical to the bibliographic curves shape (figures 11, 12 and 13).

8 VARIOUS BIBLIOGRAPHIC SIMULATIONS:

The polymer ductile solid theology corresponds to an elasto-visco plastic complex behavior [27]. In literature, various approaches were proposed to represent such a behavior: Microscopic [2, 27, 30, 31], thermodynamic [7, 27], differential [27, 32] and Macroscopic [2, 27] Approachs.

The macroscopic approach correlates better the experimental results but it is generally empirical and unidirectional. It is defined as the relation between the stress σ_{33}, deformation ε_{33}, true deformation $\dot{\varepsilon}_{33}$ and testing temperature T:

$$\sigma_{33} = \sigma_{33}(\varepsilon_{33}, \dot{\varepsilon}_{33}, T) \tag{08}$$

Where the deformation speed $\dot{\varepsilon}_{33}$ is calculated according to the relation (09):

$$\dot{\varepsilon}_{33} = \lim_{\Delta t \to 0} \frac{\Delta \varepsilon_{33}}{\Delta t} \tag{09}$$

$\Delta\varepsilon_{33}$: Variation deformation, Δt : testing time variation.

It is to be noted that the relation (08) has no sense only if the terms $\sigma_{33}, \varepsilon_{33}, \dot{\varepsilon}_{33}$ can be defined in a homogenous way in a given volume element [33] (at a small local scale in terms of the reduction dimensions, but sufficiently high to widely include the microscopic heterogeneities).

The macroscopic approach is based on a variables separation principle K_p, F and G, where : K_p: Scale factor, F : Term characterizing the stress sensitivity with respect to the deformation, G : Term characterizing the stress sensitivity with respect to the deformation speed.

The mechanical behavior laws for a macroscopic approach can be divided into two major categories:

- Multiple type law:

$$\sigma(\varepsilon_{33}, \dot{\varepsilon}_{33}) = K_p.F(\varepsilon_{33}).G(\dot{\varepsilon}_{33}) \quad (10)$$

- Additive law type:

$$\sigma(\varepsilon_{33}, \dot{\varepsilon}_{33}) = F(\varepsilon_{33}) + G(\dot{\varepsilon}_{33}) \quad (11)$$

9 MECHANICAL BEHAVIOR MODELING AT 60°C:

For our case, we have used a G'SELL multiplicative law [34], specifically for the HDPE which is formulated:

$$\sigma = K_p.[1 - \exp(-w.\varepsilon_{33})].\exp(h.\varepsilon_{33}^{\ 2}).\dot{\varepsilon}_{33}^{\ m} \quad (12)$$

Where:

w: Viscoelastic coefficient, h: Structural hardening characteristic coefficient, m: Sensitivity coefficient at deformation speed.

We have applied this relation to the experimental curve 60°C for a stretching speed 50mn/mn. A preliminary observation needs to be made regarding the way the behavior law $\sigma = \sigma(\varepsilon, \dot{\varepsilon}, T)$ in a uniaxial deformation [35] is obtained from an experimental law $\sigma_{33} = \sigma_{33}(\varepsilon_{33}, \dot{\varepsilon}_{33}, T)$ in a plain deformation. This is a common issue encountered in all the mechanical behavior studies in triaxial stress. Therefore, the objective is to define the equivalence relations allowing from the stress states and triaxial deformation $[\sigma]$, $[\varepsilon]$, $[\dot{\varepsilon}]$ to calculate the effective stresses and deformations which follow the same laws that the material solicits in a uniaxial tensile.

9.1 Stress, deformation, deformation speed equivalents calculations:

In the isotropic polymer materials [35]; it was demonstrated that Von Mises relations based on the triaxial stretchers J_2 second variant largely accounted for experimental results mainly to the moderate deformations (perfect plastic homogeneous plain deformation). The stresses, deformations and equivalent deformation speed $(\sigma_{eq}, \varepsilon_{eq}, \dot{\varepsilon}_{eq})$ are calculated according to the following relations:

$$\sigma_{eq} = \frac{\sqrt{3}}{2}\sigma_{33} \quad (13)$$

$$\varepsilon_{eq} = \frac{2}{\sqrt{3}}\varepsilon_{33} \quad (14)$$

$$\dot{\varepsilon}_{eq} = \frac{2}{\sqrt{3}}\dot{\varepsilon}_{33} \quad (15)$$

9.2 Stress, deformation, deformation speed effectives calculations:

In the various numerical studies on polymers instabilities [35, 36]; it is shown that the reduction complex geometry introduces a significant stress state disturbance whereas the local deformation state is of minor importance:

$$\sigma_{eff} \approx F_T.\sigma_{eq},\ \varepsilon_{eff} \approx \varepsilon_{eq},\ \dot{\varepsilon}_{eff} \approx \dot{\varepsilon}_{eq} \quad (16)$$

Where F_T is the coefficient of the stress triaxiality. An accurate expression of this factor is not strictly usable as it is in principle the stresses state in the reduction depends not only on its geometry, but also on the material mechanical properties [36]. F_T may be determined by the Bridgman model [37] which includes the geometrical parameters of the reduction area or by the ratio [35]:

$$F_T = \frac{\overline{\sigma_{eff}}}{\overline{\sigma_{33}}} \quad (17)$$

$\overline{\sigma_{eff}}$ and $\overline{\sigma_{33}}$ respectively represent the effective and axial stress average values in the given section. In our case, we have assumed that $F_T = 1{,}0877$ value, which has given a good accordance for the curve modeling.

9.3 Determination of modelized curve:

For simulate the experimental curve obtained by uniaxial tensile, the equation (12) takes the following form:

$$\sigma_{eff} = K_p.[1 - \exp(-w.\varepsilon_{eff})].\exp(h.\varepsilon_{eff}^{\ 2}).\dot{\varepsilon}_{eff}^{\ m} \quad (18)$$

For constant temperature values and effective deformation, the sensitivity coefficient at m deformation speed is classically achieved with the following definition:

$$m = \left.\frac{\partial \ln \sigma_{eff}}{\partial \ln \dot{\varepsilon}_{eff}}\right|_{T,\varepsilon_{eff}} \quad (19)$$

We have analyzed for deformation fixed values ε_{eff} (0.5, 0.8, 1.0), the speed influence $\dot{\varepsilon}_{\text{eff}}$ on the stress σ_{eff}. Figure 16 shows the variation of $\ln(\sigma_{eff})$ in terms of $\ln(\dot{\varepsilon}_{eff})$. We notice that this variation is linear in the explored speeds field. The slope of these curves determined by linear decrease represents the sensitivity coefficient at deformation speed m.

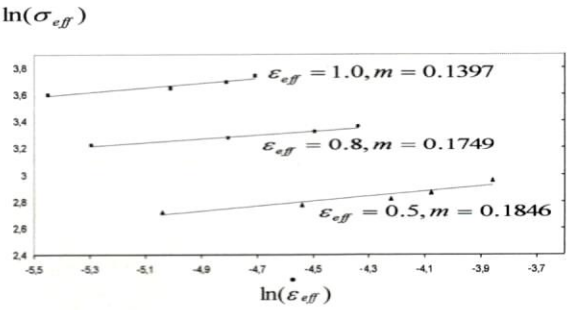

Figure 16: $\ln(\sigma_{eff})$ variation in terms of $\ln(\dot{\varepsilon}_{eff})$

The determined behaviors law parameters values (K, w, H, m) are collected in table 02. The m sample value is equal to the average of the obtained calculations $m = m_{moy} = 0{,}1664$.

Table02: Determined behaviors law parameters values for HDPE at T=60°C. s= 50mm/mn

T (°C)	s (mm/mn)	K_P (MPa)	w	H	m
60	50	42	17	0,7858	0,1664

Figures 17 and 18 respectively represent the modeled achieved from table 02 parameters, an equivalent curve and their superpositions with the effective curve.

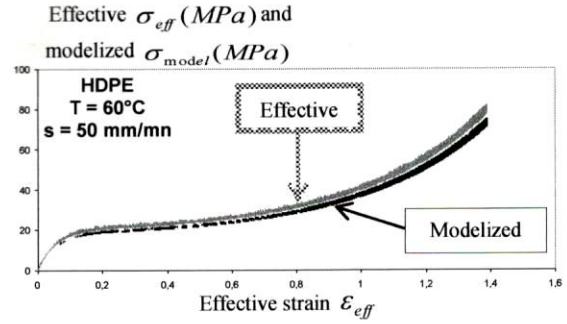

Figure 17: effective and modelized curves of high density polyethylene at 60°C

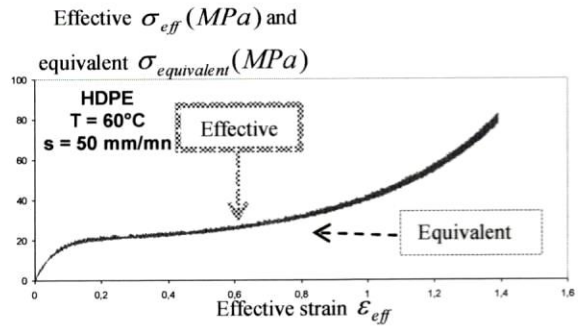

Figure 18: effective and equivalent curves of high density polyethylene at 60°C

We notice from figure 17 that there is a simulation with the effective curve. However from the curve 18 there is a simulation only at the tensile start and end, phases corresponding to the deformation homogeneity. We can notice the triaxibility coefficient importance on the curve modeling.

10. CONCLUSION:

High density polyethylene samples (HDPE) were subject to a uniaxial tensile under the influence of temperature ranging from 20 to 120°C for a constant stretching speed 50mn/mn then to various stretching speed of 50 to 800mm/mn for a constant temperature of 60°C.

1. By studying these polymer mechanical properties, we have shown the analogy of the speed increase effect and temperature decrease which have an identical effect on the material behavior along with a theoretical explanation at the macromolecular scale during the tensile testing.
2. An assumption of a relation between the nominal and true stresses $\sigma_v = \sigma_{v_2} = \sigma_n.\exp(2.\varepsilon_v)$ has given a good accordance with the bibliographic researches for a semi crystalline polymer at tensile stretching in its rubber state.
3. Assuming that the polymer is isotropic , the plain deformation , homogenous, perfect plastic and for triaxiality coefficient $F_T = 1{,}0877$, the Von Mises relations application allowed to obtain an affective curve at 60°C for s =50mm/mn.
4. A multiplicative modeling according to G'sell law has given a good compliance with the effective curve for 60°C.

11. REFERENCES:

1. G.W. Ehrenstein and F. Montagne, *Matériaux Polymères : Structure, Propriétés et Applications*, Hermès Science Publications, 2000.
2. F. Addiégo, Caractérisation de la Variation Volumique du Polyéthylène au Cours de la Déformation Plastique en Traction et en Fluage, thesis, Institut National Polytechnique de Lorraine, 2006.
3. D. Li, H. Garmestani, S. R. Kalidindi and R. Alamo, Crystallographic Texture Evolution in High Density Polyethylene During Uniaxial Tension, *polymer*, 42, pp. 4903-4913, 2001.
4. J. Rault, *Les Polymères Solides,* Edition Cepadues, Toulouse, France, 2002.
5. R. Khelif, Analyse de la Rupture et Evaluation de la Durée de Vie Basée sur la Fiabilité des Tubes en Polyéthylène pour Le Transport du Gaz, thesis, Université Blaise Pascal-Clermont II, 2007.
6. A.J Peacock, Handbook of Polyethylene "Structure, Properties and Applications", New York, NY: Marcel Dekker, 2000.
7. R. Arieby, Caractérisation Mécanique et Modélisation Thermodynamique du Comportement Anisotrope du Polyéthylène à Haute Densité. Intégration des Effets D'endommagement, thesis, Institut National Polytechnique de Lorraine (INPL), Université de Nancy, 2007.

8. R. Dossogne, Polyéthylène Haute Densité, *Technique de L'ingénieur*, DOC. A3315, pp. 1-10.
9. R.W. Warfield, Compressibility of Linear Polymers, *Journal of Applied Chemistry*, vol 17, issue 9, pp. 263-268. 1967,
10. Y. Zhao, J. Wang, Q.C.Z. Liu, M. Yang and J. Shen, High-Pressure Raman Studies of Ultra-High-Molecular-Weight Polyethylene, *Polymer Paper*, vol 31, issue 8, pp. 1425-1428, 1990.
11. C.W. Bunn, Crystal Structure of Long- Chain Normal Paraffin Hydrocarbons "Shape" of The Methylene Group, *Transaction of the Faraday Society*, vol 35, pp.482-491, 1939.
12. L. Lin and A.S. Argon, Structure and Plastic Deformation of Polyethylene, *Journal of Materials Science 29,* pp. 294-323, 1994.
13. M. Hikosaka, K. Tsukijima, S. Rastogi and A. Keller, Equilibrium Triple Point Pressure and Pressure-Temperature Phase Diagram of Polyethylene, *Polymer Physics*, vol 33, pp. 2502-2507, 1992.
14. S. Rastogi, M. Hikosaka, H. Kawataba and A. Keller, Role of Mobile Phases in The Crystallization of Polyethylene, Metastability and Lateral Growth, *Macromolecules*, vol 24, pp.6384-6391, 1991.
15. S. Rastogi, L. Kurelec and P.J. Lemstra, Crystal Size Influence in Phase Transition and Sintering of Ultrahigh Molecular Weight Polyethylene Via The Mobile Hexagonale Phase, *Macromolecules*, vol 31, issue 15, pp. 5022-5031, 1998.
16. F. Bustos, Cristallisation sous Cisaillement du Polyéthylène : Effets de L'architecture Moléculaire, thesis, Université Claude Bernard, Lyon 1 ; 2004.
17. K.E. Russell, B.K. Hunter and R.D. Heyding, Monoclinic Polyethylene Revisited, *Polymer*, vol 38, N° 6, pp. 1409-1414, 1997.
18. L. Fontana, D.Q. Vinh, M. Santaro, S. Scandalo, F.A. Gorelli, R. Binni, and M. Hanfland, High Pressure Crystalline Polyethylene Studied By X Ray Diffraction and ab Inition Simulations, *Physical Review*, vol 75, pp.174112_1-174112_11, 2007.
19. B. Taher, S. Abboudi and R. Younes, A Study of the Thermo-Elastic Damage in the Cylender of an Engine, *International Journal of Heat and Technology*, vol 28, N°2, 2010.
20. M. Madani, Structure Optical and Thermal Decomposition Characters of LDPE Graft Copolymers Synthesized by Gamma Irradiation, *Indian Academy of Sciences*, vol 33, N°1, pp. 65-73, 2010.
21. J. Cazénave, Sur Le Compromise Rigidité/ Durabilité du Polyéthylène à Haute Densité en Relation avec La Structure de Chaîne, La Microstructure et La Topologie Moléculaire Issue de La Cristallisation, thesis, Institut National des Sciences Appliquées de Lyon, 2005.
22. H.H. Kauch and E. Al, Crazing in Semicrystalline Thermoplastic, *Journal of Macromolecular Science, part B, Physics*, B38 (5-6), pp.803-815, 1999.
23. A. Peterlin, Molecular Model of Drawing Polyethylene and Polypropylene, *Journal of Material Science, B6 (6),* pp.490-508, 1971.
24. A. Yezza, Résistance à La Fissuration Sous Contraintes des Soudures des Géomembranes Polyéthylène Haute Densité, Mémoire en Science Appliquée, Ecole Polytechnique de Montréal, 2001.
25. M. Carrega and E. Coll, Matériaux Industriels, Matériaux Polymères, Edition Dunod, Paris; 2000.
26. J.M. Dorlot, J.P. Bailon and J. Masounave, Des Matériaux, Ecole Polytechnique de Montréal ; 1986.
27. F. Addiego, A. Dahoun, C. G'sell and J.M. Hiver, volume variation process of high density polyethylene during tensile and creep tests, *oil & science and technology*, rev, IFP, vol 61, pp.715-724, 2006.
28. Y. Tillier, Identification par Analyse Inverse du Comportement Mécanique des Polymères Solides, Applications Aux Sollicitations Multiaxiales et Rapides, thesis, Ecole Nationale Supérieure des Mines de Paris, 1998.
29. Ferhoum R, Etude Expérimentale et Modélisation Numérique du Comportement Mécanique du PEHD à L'état Vierge et Après Vieillissement Thermique, thesis, Université Mouloud MAMMERI de Tizi-Ouzou, Algéria, 2012.
30. A. Molinari et C. G'sell, Instabilités Plastiques Dans Les Polymères, pp. 321-344, 1995.
31. S.J.K. Ritchie, A model for the large strain deformation of polyethylene, *Journal of Materials Science*, 35, pp. 5829-5837, 2000.
32. C. G'sell and A. Dahoun, Evolution of Microstructure in Semi Crystalline Polymer under Large Deformation, *Materials Sciences and Engineering*, A175, pp. 183-199, 1994.
33. T. A. Vest, J. Amoedo and D. Lee, Effects of Thermal History, Crystallinity, and Solvent on the Transitions and Relaxations in Poly (bisphenal-A carbonate), *Journal of Polymers Sciences*, 20, pp. 141-154, 1982.
34. C. G'sell, Instabilités de Déformation Pendant L'étirage des Polymères Solides, *Revue phys. Appl.* vol 23, pp. 1085-1101, 1988.
35. M. Lucero, Etude des Instabilités d'étirage dans des Films Minces de Poly (Téréphtalate D'éthylène Glycol), thesis, Nancy, 1986.
36. P. W. Bridgman, Studies in Large Plastic Flow and Fracture, Harvard University Press, Cambridge, M.A, USA, 1964.
37. P. W. Bridgman, The Stress Distribution at The Neck of Tension Specimen, Trans. Am. Soc, Metals, vol 32, pp.553-574, 1944.